Inorganic Chemistry

Article

pubs.acs.org/IC

Structural Analysis of Isomeric Europium(III) Chelates of NB-DOTMA

Benjamin C. Webber[†] and Mark Woods*[,†,‡]

[†]Department of Chemistry, Portland State University, 1719 SW 10th Ave., Portland, Oregon 97201, United States

[‡]Advanced Imaging Research Center, Oregon Health & Science University, 3181 SW Sam Jackson Park Road, Portland, Oregon 97239, United States

Supporting Information

ABSTRACT: Water exchange in lanthanide(III) chelates is a key parameter in developing more effective MRI contrast agents. Our own efforts to optimize water exchange have focused on isolating single coordination geometries of LnDOTA-type chelates (DOTA = 1,4,7,10-tetraazacyclododecane-1,4,7,10-tetraacetate.) This isolation may be achieved by appropriately substituting the ligand framework to freeze-out the conformational exchange processes that interconvert coordination geometries. When a single nitrobenzyl substituent is used to "lock" the conformation of the macrocyclic ring, two regioisomeric chelates may be produced; the substituent may be alternatively located on the corner or the side of the ring. Here, we unambiguously demonstrate this regioisomerism by examining the COSY spectra of some conformationally locked Eu^{3+} chelates. This exercise also demonstrated that diastereoisomeric chelates arising from racemization of chiral centers during the ligand synthesis, recently discounted as the origin of multiple isomeric chelates, can be produced and isolated. Furthermore, these COSY data revealed several through space NOE correlations that afford a great deal of information about the conformation of the nitrobenzyl substituent. In those isomers in which the substituent is located on the corner of the ring, the nitrobenzyl group is oriented approximately perpendicular to the plane of the macrocycle pointing upward and away from the chelate. In contrast, when the substituent is located on the side of the ring, the nitrobenzyl group is oriented approximately in plane with the macrocycle, pointing along the side of the chelate. Because the main purpose of the nitro group is to facilitate chemical modification and conjugation to biologically relevant molecules, these differences may have important consequences. Specifically, it seems likely that the same chelate may interact very differently with biological systems and molecules depending upon the regioisomer and therefore the orientation of the chelate relative to the biomolecule.

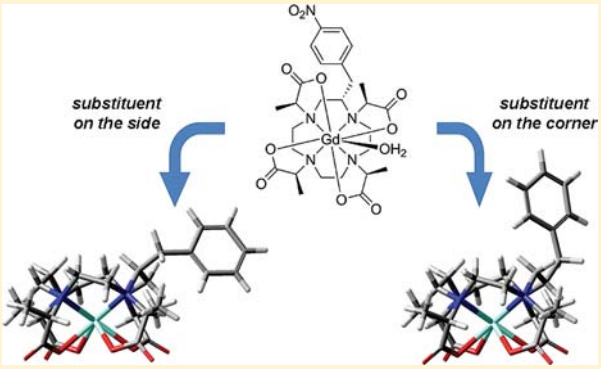

INTRODUCTION

The physical and chemical properties of chelates of Ln^{3+} ions with octadentate ligands derived from DOTA have received considerable interest over the past two and half decades primarily as a result of the use of GdDOTA as a contrast agent for MRI. GdDOTA (Chart 1) is ideal for this application primarily owing to its inertness to demetalation under physiological conditions and its "fast" water exchange kinetics.[1,2] The Gd^{3+} ion is sandwiched in the DOTA ligand between four coplanar nitrogen atoms of the macrocyclic ring and four coplanar oxygen atoms of the pendant arms.[3] The coordination sphere is then capped by a water molecule in an apical position above the four carboxylate oxygen donors. It is exchange of this water molecule with the bulk solvent that facilitates the primary mechanism by which GdDOTA is able to function as an MRI contrast agent and increase the rate of longitudinal relaxation of solvent water protons. This "inner-sphere relaxivity" can be described by Solomon, Bloembergen, and Morgan's theory of nuclear relaxation (SBM).[4−8] SBM theory shows that inner sphere relaxivity is governed by a number of parameters several of which are characteristics of the contrast agent: τ_M, the water residence lifetime; τ_R, the molecular reorientation time; r, the Gd−H distance; and T_{1e} and T_{2e}, the electron spin relaxation time constants. When τ_R is short, as is the case for low molecular weight chelates like GdDOTA, then the influence of τ_M on relaxivity is reduced. In fact, τ_M for GdDOTA (244 ns)[2] is considerably longer than is considered optimal for an MRI contrast agent, but at imaging fields,[9,10] the short τ_R value limits relaxivity and water exchange in GdDOTA is fast enough that it does not limit relaxivity.

Low molecular weight MRI contrast agents, such as GdDOTA, are administered intravenously, whereupon they diffuse through the vascular bed and into interstitial space depending upon the permeability of the vasculature. These agents are strictly extra-cellular and will accumulate to different extents throughout the body giving rise to enhanced contrast in the MR image. The extent of agent accumulation reflects the vascular properties within a region of pathology rather than any particular characteristic of the pathology itself. A new

Received: May 31, 2012
Published: July 18, 2012

   dx.doi.org/10.1021/ic3011597 | *Inorg. Chem.* 2012, 51, 8576−8582

Chart 1

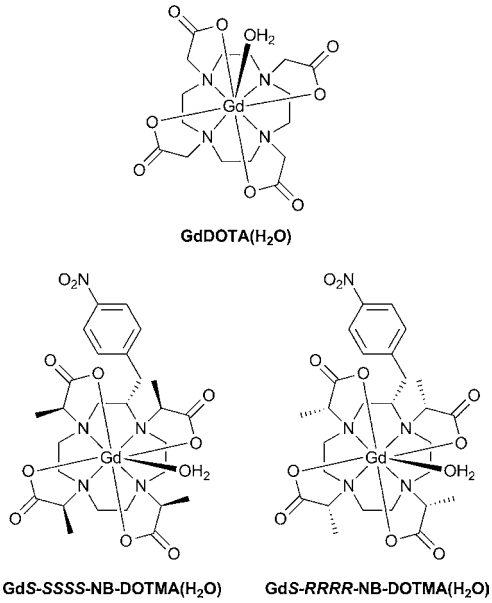

generation of contrast agent is now envisioned in which the agent is "targeted" to some physical characteristic of the pathology of interest.[11] Binding of the agent to its "target" will prolong the accumulation of the agent within the region of pathology, aiding the discrimination of diseased and healthy tissue. Given the prolonged in vivo lifetimes of at least parts of the agent dose, it is critical that the most stable Gd^{3+} chelates available are employed in any targeted imaging application; in practice, this restricts the choice of chelate to derivatives of DOTA.[12]

Binding of the agent to the "target" will have a further consequence; it will tend to increase τ_R and thereby enhance relaxivity. Relaxivity enhancements at imaging fields are observed as τ_R approaches values of the order of 1 ns. Many of the "targets" of interest are present in very low concentrations, and MRI contrast agents such as GdDOTA have relatively high detection limits. It is vital therefore that relaxivity is increased to the greatest extent possible, reducing detection limits to their minimum allowing visualization of "targets" that are present even in low concentrations. Increasing τ_R will increase relaxivity, but in suboptimally exchanging chelates such as GdDOTA, relaxivity rapidly becomes limited by τ_M. To realize the full benefits of slow molecular rotation (long τ_R), it is critical that water exchange be optimized if the highest relaxivities are to be achieved. In practice this generally means that a strategy for accelerating water exchange must be employed in any targeted imaging agent.

GdDOTA exists as a dynamic equilibrium between two distorted antiprisms in solution: the mono capped square antiprism (SAP) in which the torsional angle $\varphi = \sim 39°$, and the monocapped twisted square antiprism (TSAP) in which $\varphi = \sim 27°$.[13−15] It is now well established that the water exchange kinetics of the TSAP isomer are about 50 times faster in all DOTA-type ligand systems than those of the SAP isomer.[16−20] However, GdDOTA exists predominantly (~85%) in the more slowly exchanging SAP form.[21] We have demonstrated that it is possible to constrain the coordination geometry of GdDOTA-type chelates through substitution of the ligand.[19,20,22,23] The ligand must be substituted in such a way as to halt the intramolecular exchange processes that lead to interconversion of the two coordination isomers. This means that both the macrocyclic ring and the pendant arms must be substituted. The configuration of the chiral centers generated by substitution can be then be used to control the resulting coordination geometry; if the configurations at both the ring and the arms are the same, then a TSAP coordination isomer will result. In our conformationally locked chelates, NB-DOTMA (Chart 1), methyl substituents were introduced on each pendant arm and a nitrobenzyl substituent introduced on the macrocyclic ring.[19,20]

Nitrobenzyl substituents have been introduced into a variety of polydentate ligand systems suitable for chelating Gd^{3+}, and other rare earths,[22,24−28] and indeed, a great many of these are now commercially available. The driving force for this is the facile conversion of a nitrobenzyl substituent into an aryl isothiocyanate affording a so-called bifunctional chelator (BFC).[29,30] The rationale behind BFCs is that they provide a ready platform by which a metal chelate can be introduced onto a biologically relevant molecule, such as a targeting vector for imaging applications. As such, it would seem that our previously reported NB-DOTMA chelate, constrained to adopt the rapidly exchanging TSAP coordination isomer, would represent an ideal candidate for conversion into a BFC for targeted MR imaging. However, an unanticipated complication was recently discovered when the metal ion is introduced into these highly constrained ligand systems: two regioisomeric products are obtained; one in which the nitrobenzyl substituent is located on the corner of the ring and one in which it is located on the side of the ring (Figure 1).[31] How much of each isomeric chelate is obtained has previously been demonstrated to depend upon such reaction conditions such as the pH, reactant concentration, and metal ion.[31] However, as a general rule, the corner isomer, which was previously found to be the more stable isomer, predominates when the metal ion is Eu^{3+} or Gd^{3+}. In this article, we report the results of two-dimensional NMR studies on the Eu^{3+} chelates of some isomeric NB-DOTMA ligands providing unambiguous assignments of the chelate structure and insights into the position of the nitrobenzyl substituent in each isomer.

EXPERIMENTAL SECTION

All compounds and materials were prepared using previously described methods.[19,31] All chelates were extensively purified by reversed-phase preparative HPLC using a C18(2) luna 50 mm × 250 mm Phenomenex column, eluting at 50 mL min^{-1} using a stepwise gradient over a 26 min run according to Table 1. All NMR samples were prepared in >99.9% enriched D_2O, and the pH was not adjusted but found to lie in the region of 3−4, depending upon the concentration of the chelate (each chelate is isolated in its $HEuL(H_2O)$ form by preparative HPLC). One-dimensional ^1H NMR spectra (Supporting Information) were recorded on a Bruker Avance IIa spectrometer operating at 400.13 MHz using a 5 mm broadband probe with the temperature controlled at 278 K using the installed variable-temperature controller model 2416 with BCU-05 chiller. All spectra were referenced with the HOD at 4.7 ppm. Two-dimensional COSY data were acquired on a Bruker Avance III spectrometer operating at 600.13 MHz. The temperature was controlled using the installed variable-temperature controller model 2416 with BCU-05 chiller. A 5 mm broadband probe was used to acquire 1024 × 1024 points using 16 transients per FID. In cases where sample was limited, the SAP side isomers (Supporting Information), a 1.7 mm microprobe was employed, acquiring 1024 × 1024 points using 256 transients per FID.

dx.doi.org/10.1021/ic3011597 | Inorg. Chem. 2012, 51, 8576−8582

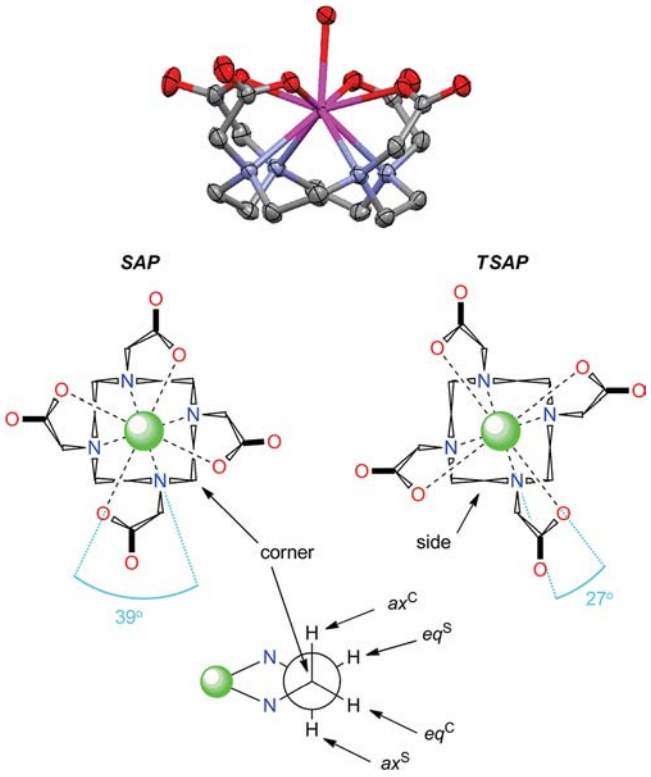

Figure 1. Structural aspects of LnDOTA-type chelates. The crystal structure of EuDOTA(H_2O) (top) showing the coordination mode. DOTA-type chelates may adopt one of two coordination geometries, SAP or TSAP (bottom), defined by the torsion angle between the two coordination planes. The notation used herein defining the corner and side positions and differentiation of macrocyclic hydrogen atoms is also presented.

Table 1. Step-Wise Solvent Gradient Used during the RP-HPLC Purification of the Chelates Studied in This Article

Time (min)	% H_2O (0.037% HCl)	% MeCN
0	78	22
3	78	22
18	65	35
20	65	35
20.1	20	80

RESULTS AND DISCUSSION

It is relatively easy to distinguish the SAP and TSAP isomers of DOTA-type chelates using a technique that probes the magnitude of the axial ligand field parameter, B_2^0, such as ^{1}H NMR or luminescence on the Eu^{3+} chelate.[32−34] The SAP isomer induces a larger B_2^0 and consequently greater splitting of the bands in the $^5D_0 \rightarrow {}^7F_1$ transition and, most germane to this discussion, larger shifts in the ^{1}H NMR spectrum. The two Eu^{3+} chelates isolated from the reaction of *S*-NB-cyclen with the *R*- alkylating agent exhibit a modest chemical shift range in the ^{1}H NMR spectrum consistent with a TSAP coordination geometry (and inversion at the pendant arm during alkylation). Initially, the production of a second chelate was attributed to racemization during alkylation of the 1-position of the macrocycle, which had been identified as the weakest nucleophile of the four macrocyclic amines.[19] However, this assignment was subsequently found to be incorrect, even ligands that had been purified to a single diastereoisomer (or that had no chiral substituent in the 1-position) were found to give rise to two isomeric TSAP chelates.[31] The nitrobenzyl group may adopt more than one position on the macrocyclic ring; of course, it must be located in an equatorial position so as to minimize torsional strain. But there are two chemically distinct carbon atoms on each ethylene bridge of the macrocycle, and in the ($\delta\delta\delta\delta$) conformation, the equatorial positions on each of these carbons afford *S*-configurations. So the nitrobenzyl substituent may locate itself on either of these carbons denoted as the side and corner positions (Figure 1). The location of the nitrobenzyl group will depend upon the direction of metal approach and the conformation of the ligand during the chelation reaction. The difference in position of the nitrobenzyl group in the two isomers of Eu*S*-*SSSS*-NB-DOTMA is unambiguously demonstrated by the 2D COSY spectra (Figures 2 and 3). 2D NMR data were acquired at 278 and 313 K; the data shown herein is exclusively that acquired at 278 K, which affords higher sensitivity and better quality spectra. No conformational changes were observed between the two temperatures.

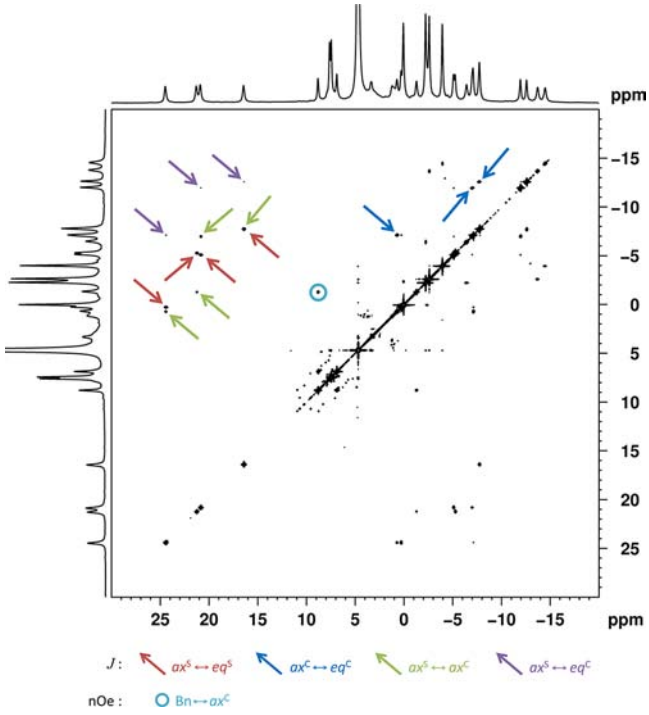

Figure 2. The ^{1}H−^{1}H correlation spectrum (COSY) of the predominant isomer of Eu*S*-*SSSS*-NB-DOTMA recorded in D_2O at 600 MHz and 278 K. *J*-coupling cross-peaks are indicated by arrows. Cross-peaks arising from NOE are indicated by circles. From the location of the cross-peaks, it can be determined that in this isomer the nitrobenzyl substituent is located on the "corner" of the macrocyclic ring.

The assignment of the ^{1}H NMR spectra of EuDOTA-type chelates is relatively easy because the axial proton located on the side carbon (ax^S) is readily identified by its large downfield shift.[35,36] Because no other protons are shifted to the same extent in this direction, this assignment is readily and unambiguously made. Each of the ax^S protons in an ethylene bridge with no substituent experiences three *J*-couplings to other protons; the strongest of these is a geminal coupling (ax^S−eq^S). There are also two vicinal couplings; on the basis of the Karplus relationship,[37] the stronger of these can be assigned

dx.doi.org/10.1021/ic3011597 | Inorg. Chem. 2012, 51, 8576−8582

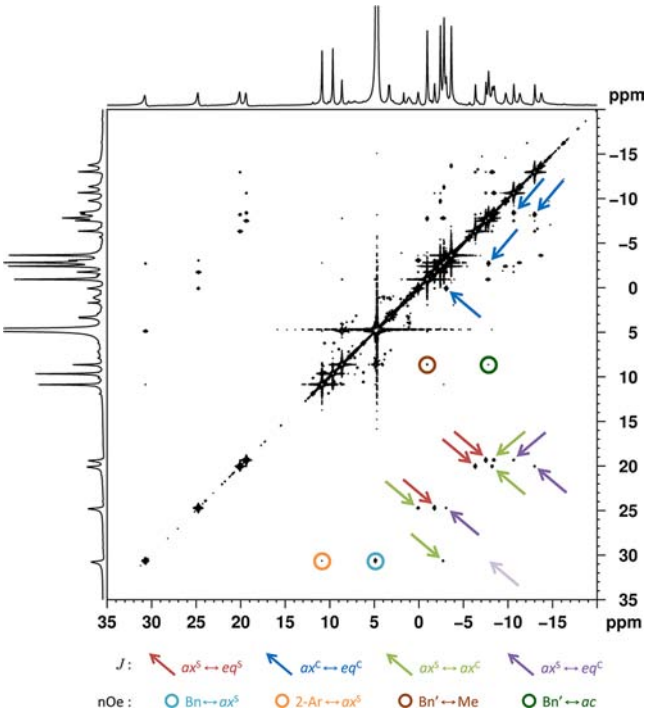

Figure 3. The ^{1}H−^{1}H correlation spectrum (COSY) of the minor isomer of Eu*S*-*SSSS*-NB-DOTMA recorded in D_2O at 600 MHz and 278 K. *J*-coupling cross-peaks are indicated by arrows; washed-out arrows indicate the expected position of a cross-peak from other coupling where the cross-peak is not actually observed. Cross-peaks arising from nOes are indicated by circles. From the location of the cross-peaks, it can be determined that in this isomer the nitrobenzyl substituent is located on the "side" of the macrocyclic ring.

to an ax^S−ax^C coupling and the weaker to an ax^S−eq^C coupling. In Figure 2, these three couplings can be identified for three ethylene bridges, identifying those as without substituent. By process of elimination, the remaining ethylene bridge must be substituted, and indeed, only two cross-peaks are observed in this case. Significantly, a geminal couple of the ax^S proton to the eq^S protons is observed but no ax^C−eq^C geminal couple, leading to the conclusion that this is indeed the substituted ethylene and that the nitrobenzyl substituent is located on the corner of the macrocycle. This conclusion is supported by one further piece of evidence. Occasionally, cross-peaks arising from the nuclear Overhauser effect (NOE) can arise in COSY spectra, and one such peak is visible in Figure 2, indicating a close spatial relationship between one of the benzylic protons and the ax^C proton of the substituted ethylene bridge.

The COSY spectrum of the other isomer of Eu*S*-*SSSS*-NB-DOTMA (Figure 3) reveals a very different coupling pattern. Again the three ethylene bridges without substituent are readily identified, as all three expected coupling cross-peaks to ax^S protons are readily identified. However, in the case of the most shifted ax^S peak, only one *J*-coupling cross-peak is observed; from its intensity, this can be assigned to an ax^S−ax^C vicinal coupling. The absence of a geminal couple to this proton clearly indicates that the nitrobenzyl substituent is located on the side of the macrocycle. This assignment is also further supported by the observation of four ax^C−eq^C geminal cross-peaks in the spectrum, indicating the presence of four eq^C protons. The spectrum is Figure 3 is notably different from that in Figure 2 in another important respect; there are many more NOE cross-peaks observed in Figure 3. Significantly, from the perspective of the substituent location, a NOE cross-peak is observed that indicates a close spatial relationship between a benzylic proton, Bn, (although that resonance is obscured by the HOD peak, this resonance may be identified by its coupling to its benzylic partner, Bn′) and the ax^S protons in this isomer, further supporting the assignment of the nitrobenzyl substituent as located on the side of the macrocycle.

One of the additional NOE cross-peaks in Figure 3 appears to indicate a close spatial relationship between the ax^S proton adjacent to the nitrobenzyl group and an ortho aromatic proton. Although this may be the case, the presence of this peak may also be explained by an NOE relay through the benzylic proton (Bn) and may not be indicative of such a close spatial relationship. Similar circumspection is due when considering the other NOE cross-peaks in this spectrum. The other benzylic proton (Bn′) appears to have two NOE correlations: one to the methyne proton (*ac*) of the pendant arm, the other with the methyl group of the same pendant arm. These peaks clearly reflect a close spatial relationship between these benzylic protons and the pendant arm but may not necessarily indicate that all three protons lie close to one another. The possibility of an NOE relay must also be considered in this case. The presence of so much NOE information in the COSY data enables some prediction of the time-averaged positions of the nitrobenzyl substituent in each chelate to be made.

On the basis of the information in Figures 2 and 3, simple MM+ geometry optimizations were undertaken to approximate the position of the nitrobenzyl substituent in each isomer. When located on the corner of the macrocycle, only one NOE cross-peak is observed in the COSY spectrum of the corner TSAP isomer (Figure 2). This suggests that the remaining protons of the substituent are positioned farther away from the chelate, and analysis places the aromatic group above the macrocyclic ring (Figure 4). In contrast, the COSY spectrum of the side TSAP isomer (Figure 3) has several NOE cross-peaks, including between a benzylic proton and protons of a pendant arm, which suggest that the nitrobenzyl substituent is pointed away from but more or less in plane with the chelate as shown (Figure 4). From this analysis, it is clear that the nitrobenzyl substituent (the envisaged point of attachment of a targeting vector) is oriented very differently depending upon whether it is located on the side or the corner of the macrocyclic ring.

Two additional considerations should be kept in mind when considering the overall picture provided by Figure 4. First, the COSY data for the side isomer (Figures 3) suggests that substitution of an ethylene bridge with a nitrobenzyl group results in significant distortion of that ethylene bridge. The vicinal ax^S−eq^C cross-peak, which is normally the weakest of the three cross-peaks, is too weak to be seen for the substituted ethylene bridges in these spectra, even though the substituent is located in the eq^S rather than the eq^C position and the corresponding cross-peaks are visible for the three other ethylene bridges. A similar observation has been previously noted in NB-DOTA chelates.[22] A likely explanation for this observation is that the ax^S−eq^C torsion angle is increased beyond the ~60° (gauche) normally observed in cyclen-based chelates. According to the Karplus relationship,[37] as this torsion angle increases, so the magnitude of the *J*-coupling decreases. This distortion is not reflected in the conformational modeling presented in Figure 4, in part because it is not possible to assess the magnitude of the distortion from the available coupling data. A further consideration is that when the temperature at which these COSY spectra are recorded is raised from 278 to

dx.doi.org/10.1021/ic3011597 | *Inorg. Chem.* 2012, 51, 8576−8582

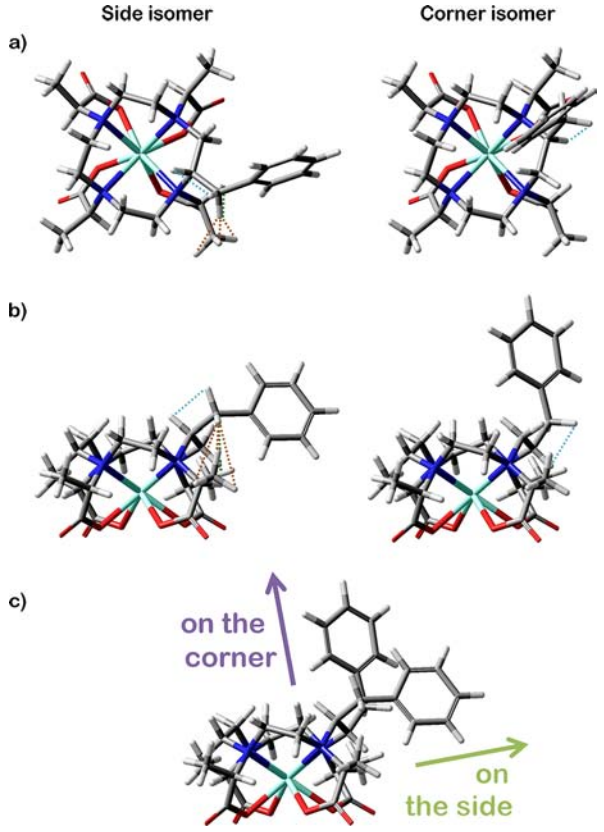

Figure 4. Models of the possible time-averaged positions of the nitrobenzyl group in Eu*S*-*SSSS*-NB-DOTMA, the TSAP isomers (a) top view and (b) side view, based upon the NOE cross-peaks in Figures 2 and 3. The observed NOEs giving rise to these predictions are indicated by dotted lines in the same color as used to identify them in Figures 2 and 3. In (c) is shown a superposition of chelates with the nitrobenzylic substituents located on the side and corner of the macrocycle, highlighting the difference in orientation. The *p*-nitro substituent of the aromatic group has been replaced by a hydrogen atom for clarity.

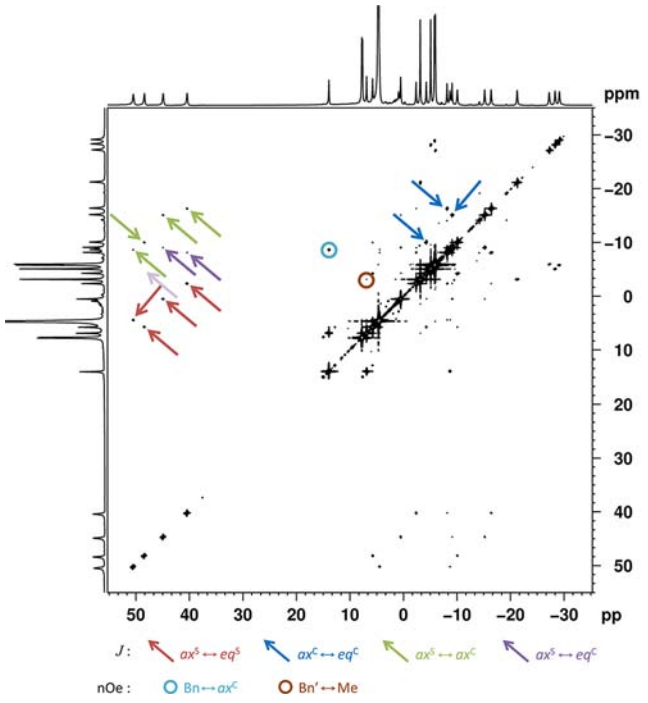

Figure 5. The ^{1}H−^{1}H correlation spectrum (COSY) of the predominant isomer isolated from the preparation of Eu*S*-*RRRR*-NB-DOTMA recorded in D_2O at 600 MHz and 278 K. *J*-coupling cross-peaks are indicated by arrows; washed-out arrows indicate the expected position of a cross-peak from other coupling where the cross-peak is not actually observed. Cross-peaks arising from NOE are indicated by circles. From the location of the cross-peaks, it can be determined that in this isomer the nitrobenzyl substituent is located on the corner of the macrocyclic ring. From the location of the cross-peaks and magnitude of the chemical shifts, it can be determined that is the corner isomer of Eu*S*-*RRRR*-NB-DOTMA.

313 K, the NOE peaks in the spectra disappear (data not shown). It seems likely that this is the result of increased intramolecular mobility of the substituent and may reflect a slightly different time-averaged structure at higher temperatures.

The preparation of the corresponding SAP isomers afforded a total of four isomeric products (all with a molecular mass of 744); the COSY spectra of the two major reaction products are shown in Figures 5 and 6. In both of these spectra the coupling patterns are consistent with the nitrobenzyl group located on the corner of the macrocyclic ring, i.e., four ax^S−eq^S geminal cross-peaks are observed but only three ax^C−eq^C cross-peaks. In each case, this assignment is supported by the observation of an NOE couple between a benzylic proton (Bn) and the ax^C proton of the substituted ethylene bridge. An NOE cross-peak between a benzylic proton (Bn′) and the methyl group of the pendant arm in the 1-position is also observed in both spectra. However, it is notable that this couple is less intense in Figure 5 (the predominant isomer) than in Figure 6, which would seem to suggest that the methyl group is somewhat nearer the Bn′ proton in the secondary corner isomer. There is also a notable difference in the shifts of this methyl group (and corresponding *ac* proton); in the predominant isomer, the shifts are comparable to those of the other pendant arms but are very different in the secondary corner isomer. These observations suggest that the configuration at the 1-position is inverted in the secondary corner isomer, which is in fact Eu*S*-*SRRR*-NB-DOTMA, the predominant isomer being the expected Eu*S*-*RRRR*-NB-DOTMA. An MM+ conformational analysis supports this conclusion; in models of the time-averaged structures (with the position of the nitrobenzyl substituent taken from the previous analysis with the TSAP isomers), the Bn′ proton appears to lie somewhat farther from the methyl group in Eu*S*-*RRRR*-NB-DOTMA than it does in Eu*S*-*SRRR*-NB-DOTMA (Figure 7).

The SAP side isomers produced during this preparation were isolated in considerably lower yields than the corresponding corner isomers.[19,31] Nonetheless, sufficient sample was obtained to allow acquisition of COSY data for each chelate confirming that side isomers were indeed produced for each ligand diastereoisomer (Figures S5 and S6, Supporting Information). In each case, the identification of just three ax^S−eq^S geminal couples but four ax^C−eq^C couples and a Bn−ax^S NOE correlation definitively support the assignment of these isomers as side isomers. In Figure S6 of the Supporting Information, the unusual shifts of the protons (methyl and *ac*) of the pendant arm in the 1-position indicate the formation of the side isomer of Eu*S*-*SRRR*-NB-DOTMA. The presence of a Bn′−*ac* NOE couple in Figure S6 of the Supporting Information provides supporting evidence for this assignment. A similar through space coupling is observed in Figure 3,

dx.doi.org/10.1021/ic3011597 | *Inorg. Chem.* 2012, 51, 8576−8582

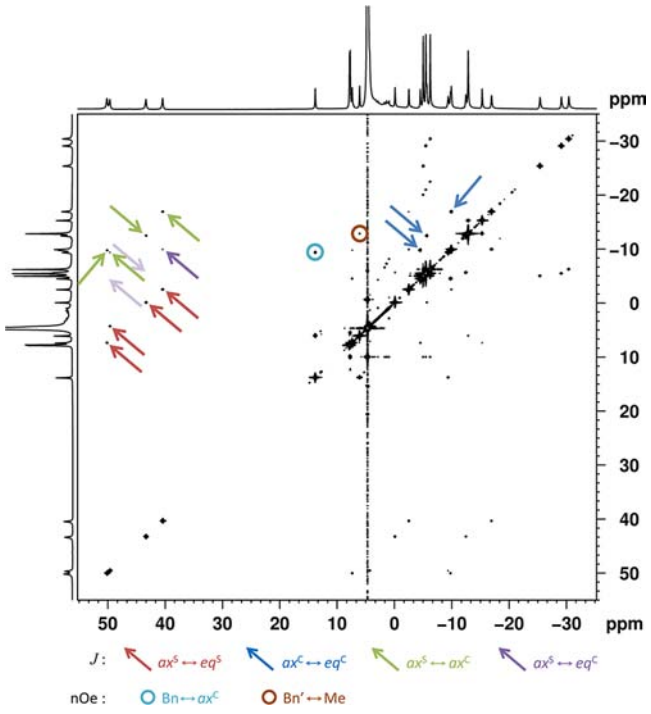

Figure 6. The $^1H-^1H$ correlation spectrum (COSY) of the second corner isomer isolated from the preparation of Eu*S-RRRR*-NB-DOTMA recorded in D_2O at 600 MHz and 278 K. *J*-coupling cross-peaks are indicated by arrows; washed-out arrows indicate the expected position of a cross-peak from other coupling where the cross-peak is not actually observed. Cross-peaks arising from NOE are indicated by circles. From the location of the cross-peaks and magnitude of the chemical shifts, it can be determined that is the corner isomer of Eu*S-SRRR*-NB-DOTMA.

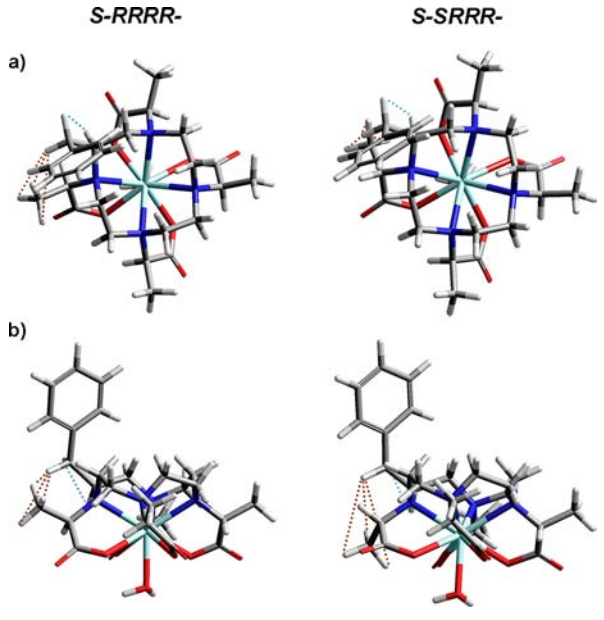

Figure 7. Models of the possible time-averaged positions of the two "corner" isomers isolated from the preparation of Eu*S-RRRR*-NB-DOTMA, both SAP isomers; (a) top view and (b) side view, based upon the NOE cross-peaks in Figures 5 and 6. The observed NOEs giving rise this these predictions are indicated by dotted lines in the same color as used to identify them in Figures 5 and 6. The *p*-nitro substituent of the aromatic group has been replaced by a hydrogen atom for clarity.

strongly suggesting that the nitrobenzyl group is oriented similarly in all side isomers, either SAP or TSAP, and in all corner isomers, either SAP or TSAP. This time-averaged positioning would account for the NOE cross-peaks observed in the *S-RRRR-* and *S-SRRR-* isomers of EuNB-DOTMA (Figure 7).

CONCLUSIONS

The COSY data presented herein provide three insights into the structure and conformation of geometrically rigid Ln^{3+} chelates derived from nitrobenzyl cyclen. They unambiguously demonstrate that the nitrobenzyl substituent of NB-DOTMA chelates may adopt a position either on the side or on the corner of the macrocyclic ring as previously postulated.[31] This regioisomerism does not occur in the more flexible LnNB-DOTA chelates in which the nitrobenzyl substituent is located on the corner of the macrocyclic ring[22] but may be an explanation for the observations of Schlesinger et al. in Cu^{2+} NB-NOTA chelates.[38] From the NOE cross-peaks that arise in these COSY spectra, it is possible to approximate the time-averaged position of the nitrobenzyl group and therefore the relative position of any group subsequently bound to the chelate through it. In the two distinct regioisomeric chelates (side versus corner), the nitrobenzyl substituent is oriented very differently with respect to the chelate. The corner isomer positions the nitrobenzyl substituent in such a way that it lies beyond the plane of the macrocyclic ring, pointing away from the chelate. Any group attached through the aromatic substituent of this chelate will lie on the opposite side of the macrocyclic ring from the open face of the metal ion. In contrast, the side isomer places the nitrobenzyl substituent roughly along the equatorial plane of the chelate, pointing out of the side of the chelate. Any group attached through the aromatic substituent of this chelate will lie adjacent to the side of the chelate. This has potential significant implications for the use of these chelates in targeted applications in which a targeting ligand is attached to the chelate through the benzylic group. The resulting conjugates will have differently oriented chelates depending upon whether the substituent is located on the side or the corner of the macrocyclic ring. This could reasonably be expected to alter the interactions (steric and electronic) between the chelate portion of the conjugate and the targets, affecting the binding mode and affinity of the conjugate.

On the basis of the results of studies on LnNB-DOTA chelates,[22] it was expected that our initial experiments would afford single isomeric chelates. The production of multiple isomeric chelates with the same coordination geometry was

Chart 2

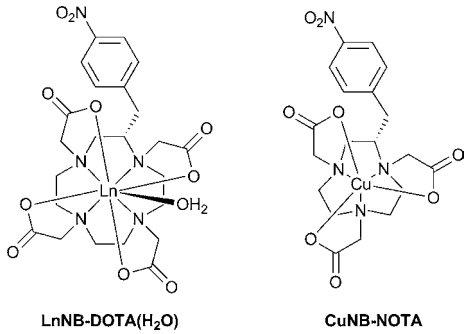

dx.doi.org/10.1021/ic3011597 | Inorg. Chem. 2012, 51, 8576–8582

originally attributed to the poor nucleophilicity of the amine in the 1-position of the macrocycle. It was thought that this poor nucleophile gave rise to a large amount of S_N1 character to the alkylation at this site and thus to some racemisation of the α-chiral center.[19] As evidence grew that multiple regioisomeric chelates were being produced as the metal ion was introduced to the ligand, this explanation was revised.[31] The results of these COSY experiments unambiguously demonstrate that in fact both explanations are correct: in the preparation of the ligand, racemisation of the α-chiral center at the 1-position may occur producing a *SRRR*- or *RSSS*-byproduct; in preparation of the chelate, two different regioisomers of the chelate will be produced depending upon the direction of approach of the metal ion and the conformation of the ligand at the instant of initial reaction, affording either a side or a corner regioisomer.

■ ASSOCIATED CONTENT

Ⓢ Supporting Information

Full assignments of each ^{1}H NMR spectrum, COSY spectra, and conformational analyses of the side isomers of Eu*S*-*RRRR*-NB-DOTMA and Eu*S*-*SRRR*-NB-DOTMA. This material is available free of charge via the Internet at http://pubs.acs.org

■ AUTHOR INFORMATION

Corresponding Author

*E-mail: woodsmar@ohsu.edu or mark.woods@pdx.edu. Phone: + 1 503 725 8238 or + 1 503 418 5530.

Notes

The authors declare no competing financial interest.

■ ACKNOWLEDGMENTS

The author thanks the National Institutes of Health (EB-11687), Oregon Nanoscience and Microtechnology Institute (N00014-11-1-0193), and Oregon Opportunity for Biomedical Research for financial support

■ REFERENCES

(1) Toth, E.; Brücher, E.; Lazar, I.; Toth, I. *Inorg. Chem.* **1994**, *33*, 4070.
(2) Powell, D. H.; Ni Dhubhghaill, O. M.; Pubanz, D.; Helm, L.; Lebedev, Y. S.; Schlaepfer, W.; Merbach, A. E. *J. Am. Chem. Soc.* **1996**, *118*, 9333.
(3) Meyer, M.; Dahaoui-Gindrey, V.; Lecomte, C.; Guilard, L. *Coord. Chem. Rev.* **1998**, *180*, 1313.
(4) Bloembergen, N. *J. Chem. Phys.* **1957**, *27*, 572.
(5) Bloembergen, N.; Morgan, L. O. *J. Chem. Phys.* **1961**, *34*, 842.
(6) Bloembergen, N.; Purcell, E. M.; Pound, R. V. *Phys. Rev.* **1948**, *73*, 679.
(7) Solomon, I. *Phys. Rev.* **1955**, *99*, 559.
(8) Solomon, I.; Bloembergen, N. *J. Chem. Phys.* **1956**, *25*, 261.
(9) Caravan, P.; Ellison, J. J.; McMurry, T. J.; Lauffer, R. B. *Chem. Rev.* **1999**, *99*, 2293.
(10) Toth, E.; Helm, L.; Merbach, A. E. In *Chemistry of Contrast Agents in Medical Magnetic Resonance Imaging*; Toth, E., Merbach, A. E., Eds.; Wiley: New York, 2001.
(11) Welch, M. J.; Eckelman, W. C.*Targeted Molecular Imaging*; Taylor & Francis: Boca Rotan, 2012.
(12) Sherry, A. D.; Caravan, P.; Lenkinski Robert, E. *J. Magn. Reson. Imag.* **2009**, *30*, 1240.
(13) Aime, S.; Botta, M.; Ermondi, G. *Inorg. Chem.* **1992**, *31*, 4291.
(14) Hoeft, S.; Roth, K. *Chem. Ber.* **1993**, *126*, 869.
(15) Desreux, J. F. *Inorg. Chem.* **1980**, *19*, 1319.
(16) Aime, S.; Barge, A.; Bruce, J. I.; Botta, M.; Howard, J. A. K.; Moloney, J. M.; Parker, D.; de Sousa, A. S.; Woods, M. *J. Am. Chem. Soc.* **1999**, *121*, 5762.
(17) Dunand, F. A.; Aime, S.; Merbach, A. E. *J. Am. Chem. Soc.* **2000**, *122*, 1506.
(18) Woods, M.; Aime, S.; Botta, M.; Howard, J. A. K.; Moloney, J. M.; Navet, M.; Parker, D.; Port, M.; Rousseaux, O. *J. Am. Chem. Soc.* **2000**, *122*, 9781.
(19) Woods, M.; Botta, M.; Avedano, S.; Wang, J.; Sherry, A. D. *Dalton Trans.* **2005**, 3829.
(20) Woods, M.; Kovacs, Z.; Zhang, S.; Sherry, A. D. *Angew. Chem., Int. Ed.* **2003**, *42*, 5889.
(21) Aime, S.; Botta, M.; Fasano, M.; Marques, M. P. M.; Geraldes, C. F. G. C.; Pubanz, D.; Merbach, A. E. *Inorg. Chem.* **1997**, *36*, 2059.
(22) Woods, M.; Kovacs, Z.; Kiraly, R.; Bruecher, E.; Zhang, S.; Sherry, A. D. *Inorg. Chem.* **2004**, *43*, 2845.
(23) Howard, J. A. K.; Kenwright, A. M.; Moloney, J. M.; Parker, D.; Woods, M.; Port, M.; Navet, M.; Rousseau, O. *Chem. Commun.* **1998**, 1381.
(24) Brechbiel, M. W.; Gansow, O. A.; Atcher, R. W.; Schlom, J.; Esteban, J.; Simpson, D.; Colcher, D. *Inorg. Chem.* **1986**, *25*, 2772.
(25) Camera, L.; Kinuya, S.; Garmestani, K.; Wu, C.; Brechbiel, M. W.; Pai, L. H.; McMurry, T. J.; Gansow, O. A.; Pastan, I.; Paik, C. H.; et al. *J. Nucl. Med.* **1994**, *35*, 882.
(26) Ruloff, R.; Toth, E.; Scopelliti, R.; Tripier, R.; Handel, H.; Merbach, A. E. *Chem. Commun.* **2002**, 2630.
(27) Laus, S.; Ruloff, R.; Toth, E.; Merbach, A. E. *Chem.—Eur. J.* **2003**, *9*, 3555.
(28) Tircso, G.; Benyo Eniko, T.; Suh Eul, H.; Jurek, P.; Kiefer Garry, E.; Sherry, A. D.; Kovacs, Z. *Bioconjug. Chem.* **2009**, *20*, 565.
(29) Frullano, L.; Caravan, P. *Curr. Org. Synth.* **2011**, *8*, 535.
(30) Lattuada, L.; Barge, A.; Cravotto, G.; Giovenzana, G. B.; Tei, L. *Chem. Soc. Rev.* **2011**, *40*, 3019.
(31) Tircso, G.; Webber, B. C.; Kucera, B. E.; Young, V. G.; Woods, M. *Inorg. Chem.* **2011**, *50*, 7966.
(32) Muller, G.; Kean, S. D.; Parker, D.; Riehl, J. P. *J. Phys. Chem. A* **2002**, *106*, 12349.
(33) Dickins, R. S.; Parker, D.; Bruce, J. I.; Tozer, D. J. *Dalton Trans.* **2003**, 1264.
(34) Borel, A.; Bean, J. F.; Clarkson, R. B.; Helm, L.; Moriggi, L.; Sherry, A. D.; Woods, M. *Chem.—Eur. J.* **2008**, *14*, 2658.
(35) Ren, J.; Zhang, S.; Sherry, A. D.; Geraldes, C. F. G. C. *Inorg. Chim. Acta* **2002**, *339*, 273.
(36) Marques, M. P. M.; Geraldes, C. F. G. C.; Sherry, A. D.; Merbach, A. E.; Powell, H.; Pubanz, D.; Aime, S.; Botta, M. *J. Alloy. Compd.* **1995**, *225*, 303.
(37) Karplus, M. *J. Am. Chem. Soc.* **1963**, *85*, 2870.
(38) Schlesinger, J.; Rajander, J.; Ihalainen, J. A.; Ramesh, D.; Eklund, P.; Fagerholm, V.; Nuutila, P.; Solin, O. *Inorg. Chem.* **2011**, *50*, 4260.